Leaded Brass Rods C 38500 for Automatic Machining Operations: A Technical Report

G. Pantazopoulos

(Submitted 20 August 2001; in revised form 2 April 2002)

C 38500 is a widely used copper alloy with a great variety of applications from decoration and architecture to mechanical/electrical engineering. The chemical composition of this alloy offers superior machinability and subsequently increased productivity in high-speed machining and manufacturing processes. In European countries, this alloy is used primarily as free cutting brass (CW 614N according to EN 12164: 1998), similar to C 36000 alloy, which is used also for thread rolling. The lower percentage of Cu compared to C 36000 (nominal 58% instead of 61%) decreases the cost of the raw materials. This paper reports the principal aspects of microstructure, mechanical properties, and machinability of this alloy in relation to the industrial manufacturing process used.

Keywords C 38500 copper alloy, high-speed machining, machinability

1. General Alloy Chemical Composition and Manufacturing Processes

1.1 Brass Rod Production

The chemical composition of the C 38500 varies within the ranges given in ASTM B-455 standard specification: Copper-Zinc-Lead Alloy (Leaded Brass) Extruded Shapes (Table 1).[1]

Alloy C 38500 serves as raw material for the production of various products ranging from decoration to mechanical/electrical engineering. Housewares, kitchen utensils, knobs and door handles, fireplace parts, nuts and screws, fittings for plumbing installations, precision parts for electrical/mechanical equipment, and many other micro-components are produced from this alloy. The production of the final parts is accomplished by high-speed machining (turning) of leaded brass-C 38500 rods. Various other shapes (e.g., profiles) can be also produced, but the most popular shapes for machining operations are round and hexagonal rods. Lead (2.5-3.5%), precipitated in a fine and homogeneous distribution, serves as a chip-breaking constituent, increasing the machinability of the material and the cutting-tool life.

Brass rods of the C 38500 alloy (HALCOR 583 alloy) are produced by using classical casting and metal-forming operations, followed by heat treatment where necessary. A typical flow chart showing the sequence of the manufacturing operations of brass rods is shown in Fig. 1. Continuous melting and casting is the first stage for the production of round brass billets. The next stage is hot billet extrusion. Preheating of the billets up to 650-750 °C, depending on the alloy chemical composition and extrusion ratio (R), is required as the hot workability of the β-phase is increased.[2] Subsequent pickling in sulfuric acid bath and rinsing in subsequent water baths is used for surface cleaning of the extruded bars. The dimensional tolerances and the hardness requirements are achieved by subsequent one-pass cold-drawing with a reduction ratio (r_T) up to 10%, resulting in work hardening and subsequent surface strengthening, contributing to overall bar mechanical strength and also protecting the surface from mechanical damages (fric-

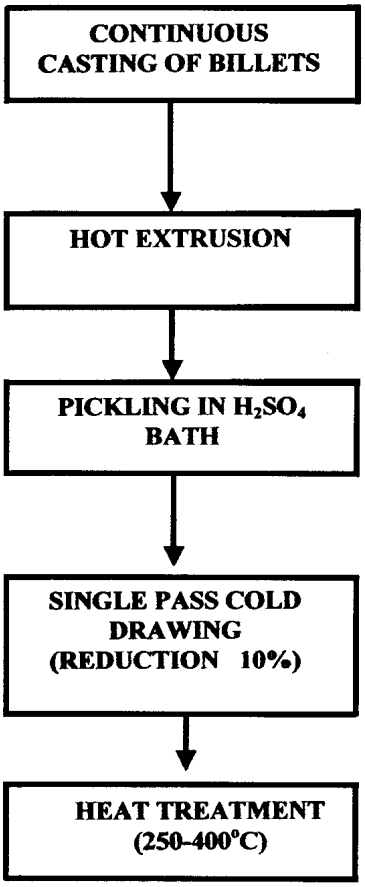

Fig. 1 A simplified flow chart showing the production sequence of brass rods

G. Pantazopoulos, HALCOR S.A. Metal Works, Quality Control Department, 252 Piraeus Street, 17778 Athens, Greece. Contact e-mail: gpantaz@halcor.vionet.gr.

Table 1 Chemical Composition Ranges (wt.%) of C 38500 (According to ASTM B-455)

Cu	Pb	Fe	Zn
55.0-59.0	2.5-3.5	0.35 max	Rem

Table 2 Chemical Composition (wt.%) of the 8 mm Diameter Brass Rods C 38500

Cu	Pb	Sn	Ni	Fe	Al	Bi	Sb	Zn
58.75	3.04	0.061	0.020	0.169	0.015	0.0011	0.0017	Rem

tion, abrasion, etc.). Heat treatment, mainly stress relief (250-400 °C), is necessary to eliminate the residual stresses originating mainly from cold metal forming. However, stress-relieving annealing is quite often required to prevent environmental failures like stress-corrosion cracking.[3]

1.2 Chemical Composition Influence

Very careful on-line control of the impurities in the melting furnace is necessary to avoid serious formation defects. Bismuth (Bi) leads to the formation of brittle intergranular films, giving rise to hot shortness effects and therefore deteriorating the hot workability of the alloy. On the other hand, antimony (Sb) impairs the alloy cold workability.[4,5] The (α+β)-brasses and β-brasses are more suitable than α-brasses for extrusion of complex shapes because of the lower extrusion temperatures and extrusion loads. The fraction of β-phase has a significant effect on the hot extrudability and can be controlled by adding certain alloying elements. The hot extrudability is improved by increasing the β-phase content. This means that for a given press load and extrusion ratio, the extrusion temperature can be decreased. The zinc (Zn) equivalence factor or Zn equivalent of an element aids in understanding how the β-phase content is modified by the addition of this element in the alloy. In particular, these elements, which have positive Zn equivalence factor, increase of the β-phase content (equivalent to increasing the Zn content) while those that have negative Zn equivalence factor or Zn equivalent decrease the β-phase content in the alloy (equivalent to decreasing the Zn content). The addition of 1% of the alloying element has the same effect on the microstructure as the percentage of Zn given as the Zn equivalent. The majority of the elements reported possess positive a Zn equivalent, and only nickel (Ni) has negative Zn equivalent (ranging from −0.9 to −1.5; average −1.2),[6,7] which is equivalent to saying that 1% Ni addition is the same as having an alloy with 1.2% less Zn.

Ni and tin (Sn) mass fractions must be kept below 0.3% due to the associated strain-hardening effects during cold working.

2. Lab Testing of Microstructure and Mechanical Properties

2.1 Microstructure

The materials under study were rods 8 mm in nominal diameter. The chemical composition of the rods was determined by means of x-ray-fluorescence (XRF) and optical emission spectroscopy (OES) using ARL 8680 and 4460 models, respectively (Table 2).

A typical metallographic procedure was employed for sample preparation: the sample was polished to a 4000-grade silicon carbide paper and then finished with an alumina suspension (0.25 and 0.1 μm respectively). The typical microstructure of this alloy consists of α+β phases; the α phase is the copper solid solution with zinc, having a face-centered-cubic crystal lattice, while the β phase is the ordered nonstoichiomet-

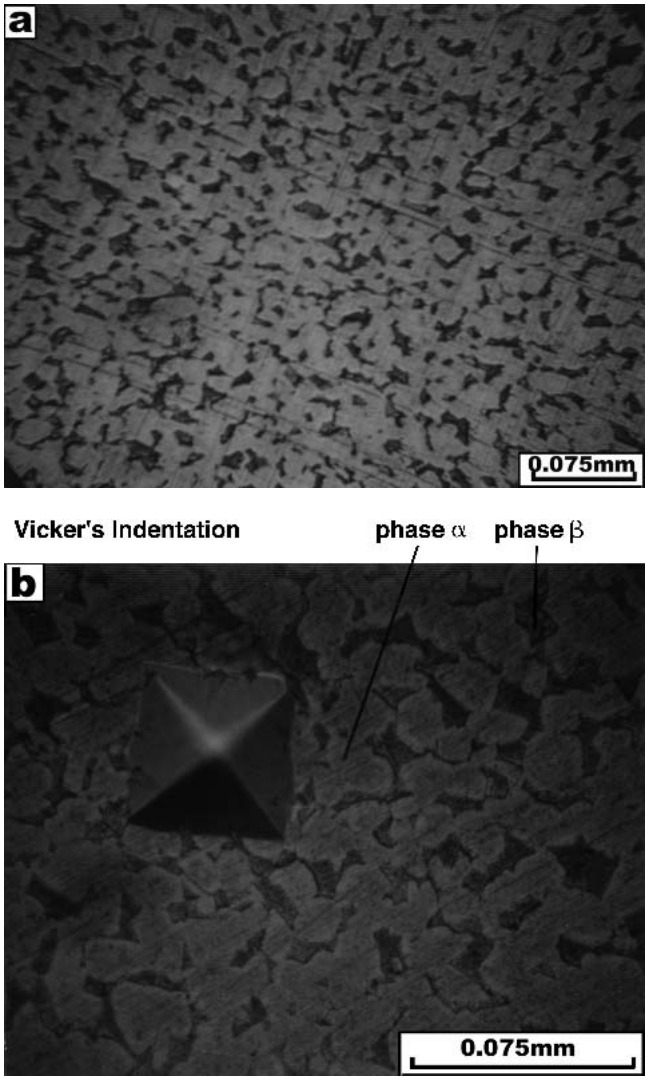

Fig. 2 **(a)** Optical micrograph showing the α+β microstructure of C 38500; **(b)** detail of Fig. 2(a)

Table 3 Room-Temperature Mechanical Properties of the 8 mm Diameter Brass Rods C 38500

Brass rod	Hardness, HRB	Tensile Strength, UTS, MPa/ksi	Elongation, A, %
Diameter, 8 mm C38500	83	486/70	11.0

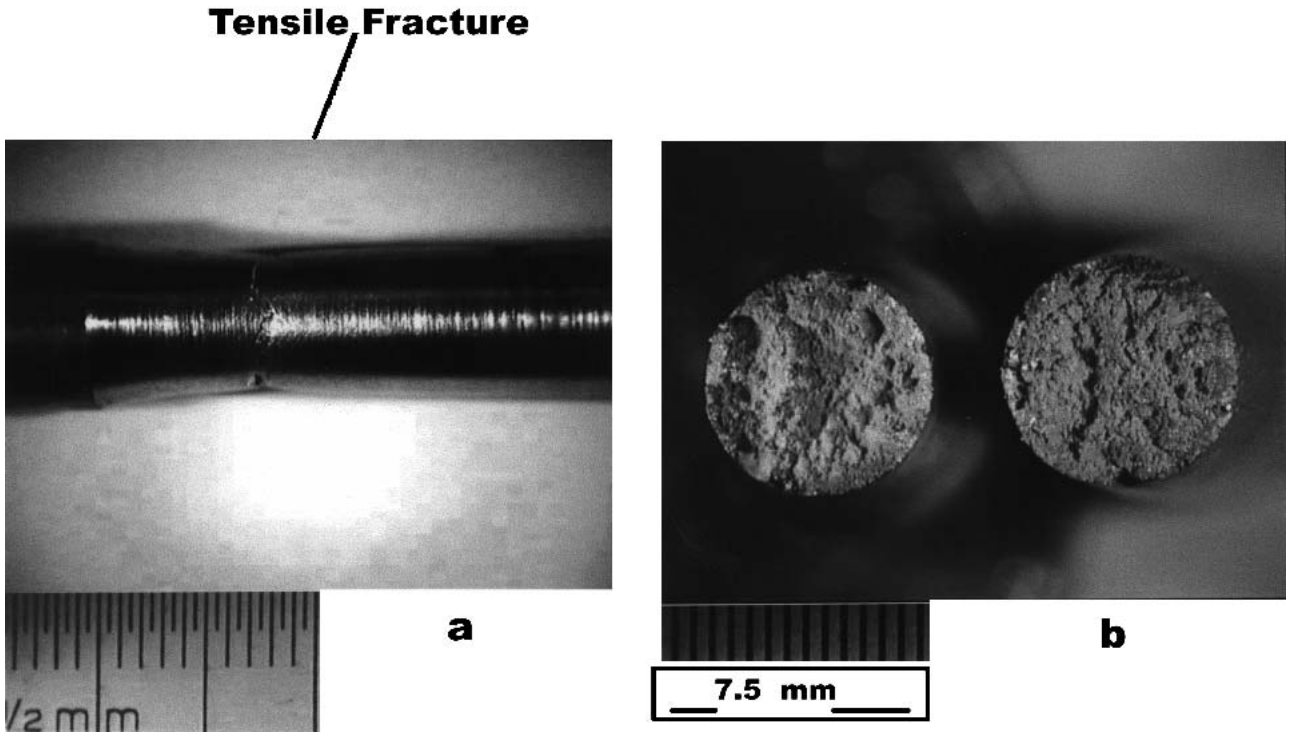

Fig. 3 **(a)** Tensile fracture (after tensile test); **(b)** related fracture surfaces

ric compound CuZn with a body-centered-cubic (bcc) lattice. The microstructure of the drawn rod is presented in Fig. 2. Ferric chloride ($FeCl_3$) solution was used as an etching reagent for 10 s to reveal the phase morphology.

2.2 Mechanical Properties

The temper (or the metallurgical condition) and the associated mechanical properties of the drawn rods were those typical of half-hard material. The hardness of the rod was measured in the cross-section midway between the outer surface and the central axis of specimen, using an Ernst AT200 bench hardness tester. The specimen was polished with an 800-grade silicon carbide paper before hardness testing. The Rockwell B method was employed for hardness measurement, using a 1/16 in. steel ball indenter and 100 kp (981 N) applied load, according to ASTM E-18 standard specification. The tensile properties of the rod were determined using an Amsler 15 ton hydraulic tension machine according to ASTM E-8 standard specification. The macroscopic room temperature mechanical properties are listed in Table 3.

Increased ductility was observed prior to fracture by the formation of localized neck. The subsequent fracture was ductile, and the resultant surfaces were sufficiently rough, consisting of interconnected shear cracks (Fig. 3).

Cold drawing as the final metal forming operation led to hardness inhomogenities due to heterogeneous plastic deformation between the surface and core material. However, moderate reductions up to 14% maximum tended to minimize the hardness differences and the associated residual stresses. Microhardness measurements, using Vickers diamond indenter and a 0.5 kp (4.905 N) applied load, indicated a surface microhardness up to 168 $HV_{0.5}$ while the core (center) microhardness was found to equal 158 $HV_{0.5}$.

3. Machinability

The machinability of the rods was evaluated by microstructural/morphological study using scanning electron microscopy (SEM) and by conducting preliminary machining experiments.

Lead (Pb) content and Pb particle dispersion played an important role in the machining capability of the material. Pb remained insoluble to the α or β phase and it was distributed along the present (or former) grain boundaries. As the Pb particle distribution became finer (less than 5 μm) and more homogeneous, the chip-breaking action during cutting processes became stronger, and therefore the machinability was enhanced. The formation of small and broken chip has mainly the following advantages:

- Ease of machining operation; maximum productivity,
- Lower cutting forces,
- Better surface finish of the workpiece,
- Closer tolerances of the final component, and
- Less tool wear—longer tool life.

The Pb dispersion was revealed using backscattered electron (BSE) imaging in SEM (Fig. 4a,b). Pb was present in the

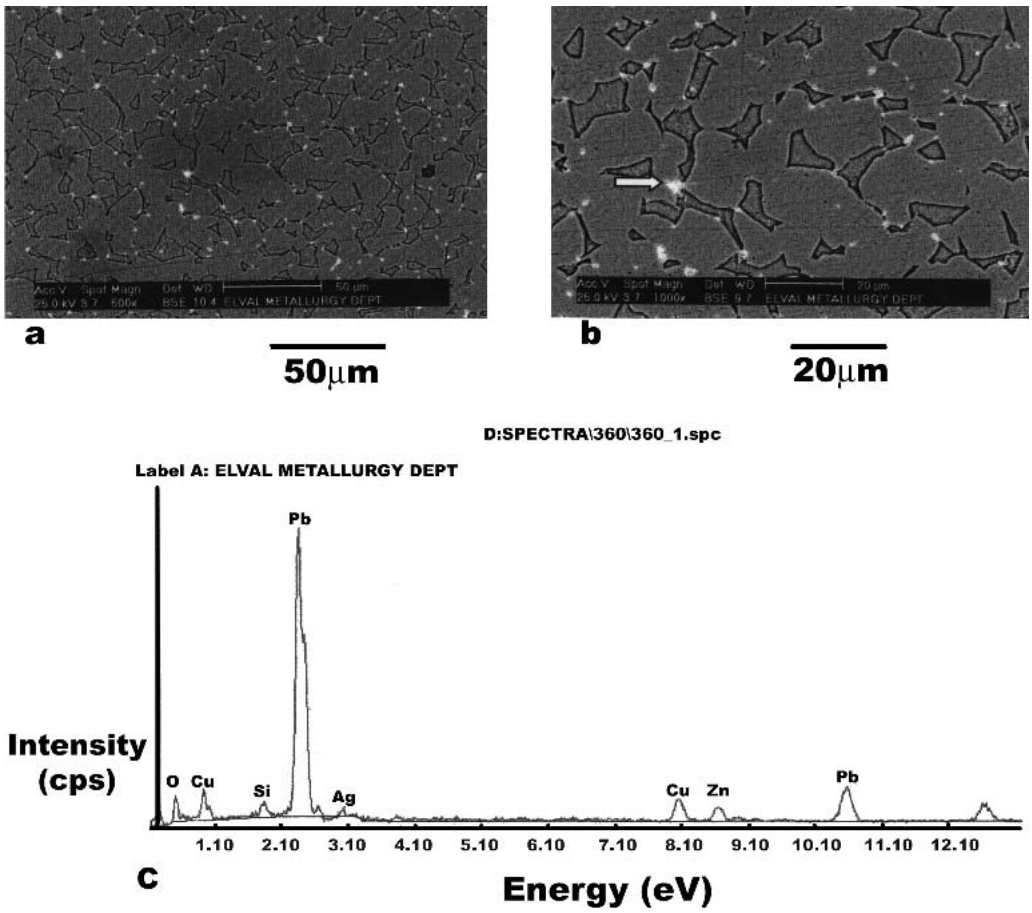

Fig. 4 **(a)** SEM micrograph of the polished and etched cross-section, showing the Pb dispersion in the dual-phase microstructure; **(b)** detail of Fig 4(a); **(c)** EDS spectrum taken on the arrow position

form of light spherical particles (0.7-4.0 μm) analyzed also by energy dispersive spectrometry (EDS); see Fig. 4(c).

The preliminary machinability tests were based on the observation of chip size/geometry and morphology by varying the cutting parameters. A classical turning operation was selected as the most representative industrial test in the attempt to simulate the behavior of the material processed subsequently on automatic turning machines. The turning speed was up to 395 rpm (the linear speed was up to 0.165 m/s) using cemented tungsten carbide insert as a cutting tool. Figure 5 shows the various chip geometries and sizes for the corresponding turning parameters. The chip size tended to increase by increasing the depth of cut, while no appreciable changes were recorded by changing the feed rate. The depth of cut was constant within the turning cycle (i.e., 0.4, 1.0, or 3.0 mm). The horizontal advancement of the tool per revolution is given by the value of the feed rate (0.25 or 0.50 mm/rev).

Morphological observations of the produced chips, using optical metallography, indicated the absence of flow-zone (Fig. 6). Segmented chips with intense shear fractures were produced during turning as a result of bi-phase microstructure (α+β) and the presence of Pb.[8] Pb also decreased friction and temperature at the tool-workpiece interface, therefore increasing the tool life. Various aspects of machinability can be found in Ref. 9 and 10.

4. Conclusions

C 38500 brass rods are used for a wide range of applications from architectural and decorative article fabrication (e.g., door handles, knobs, kitchen/fireplace utensils, etc.) to mechanical and electrical engineering (screws, nuts, pressure valves, fittings, electrical components, etc.) by using high-speed machining processes.

The microstructure consists of α+β phases and uniformly dispersed Pb particles. The Pb dispersion and size (mainly less than 1 μm) plays an important role to the machinability of the alloy. The chip size/geometry and morphology was studied in preliminary turning tests, which showed an incremental tendency of chip size with depth of cut, but no appreciable changes were observed with feed rate variation. Intense fracturing and absence of flow zone were observed in metallographic section of the produced rods.

Acknowledgments

The author wishes to thank Dr. Mavropoulos, Dr. Patsiogiannis, and Mr. Spathis from ELVAL Metallurgy Department, and Mr. Galatis from HALCOR Quality Control Department for their valuable contribution to the completion of the experimental work.

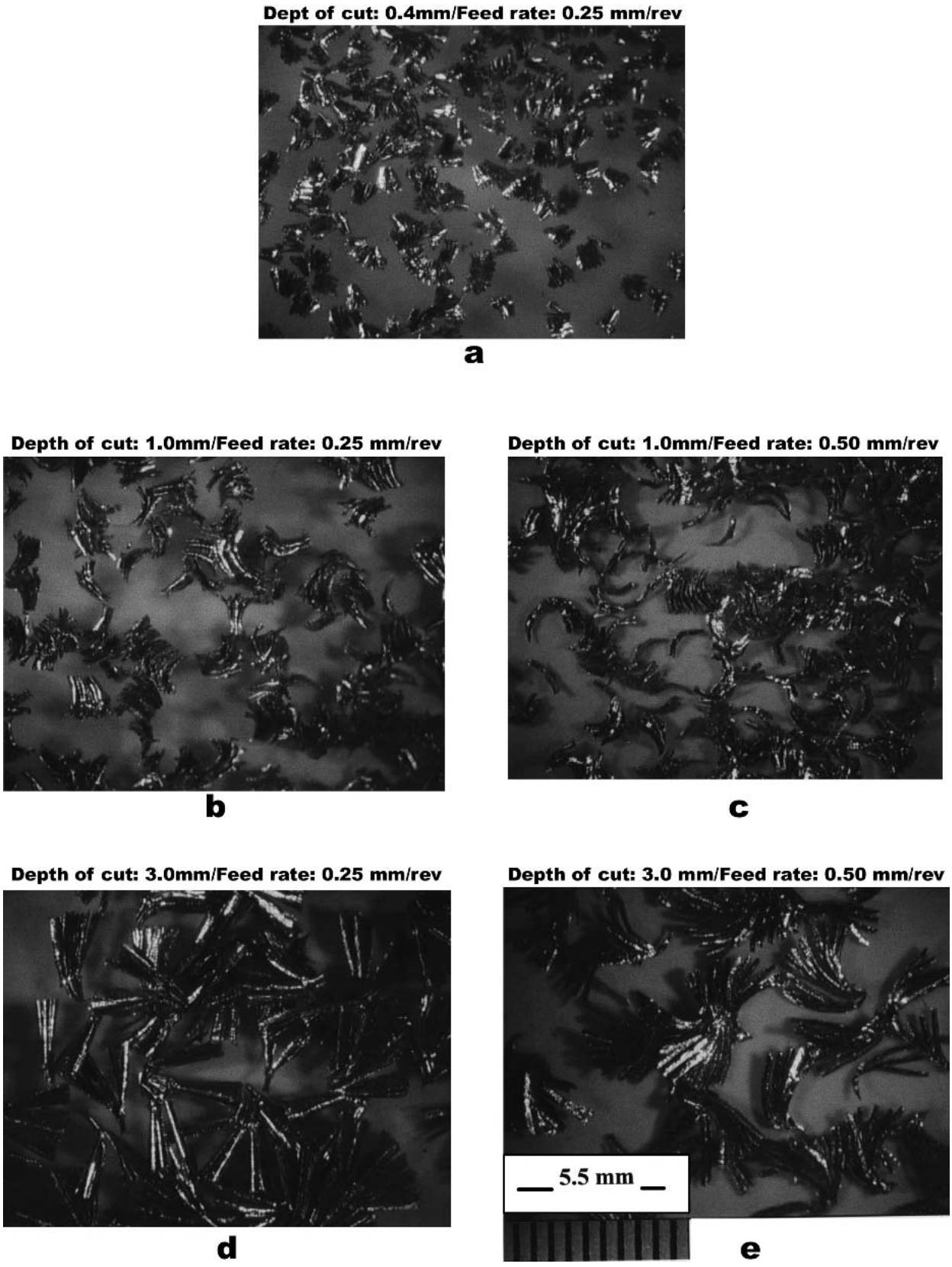

Fig. 5 Chip size and geometry in relation to turning parameters (cutting speed is constant up to 0.165 m/s): **(a)** depth of cut: 0.4 mm, feed rate: 0.25mm/rev; **(b)** depth of cut: 1.0 mm, feed rate: 0.25 mm/rev; **(c)** depth of cut: 1.0 mm, feed rate: 0.50 mm/rev; **(d)** depth of cut: 3.0 mm, feed rate: 0.25 mm/rev; **(e)** depth of cut: 3.0 mm, feed rate: 0.50 mm/rev

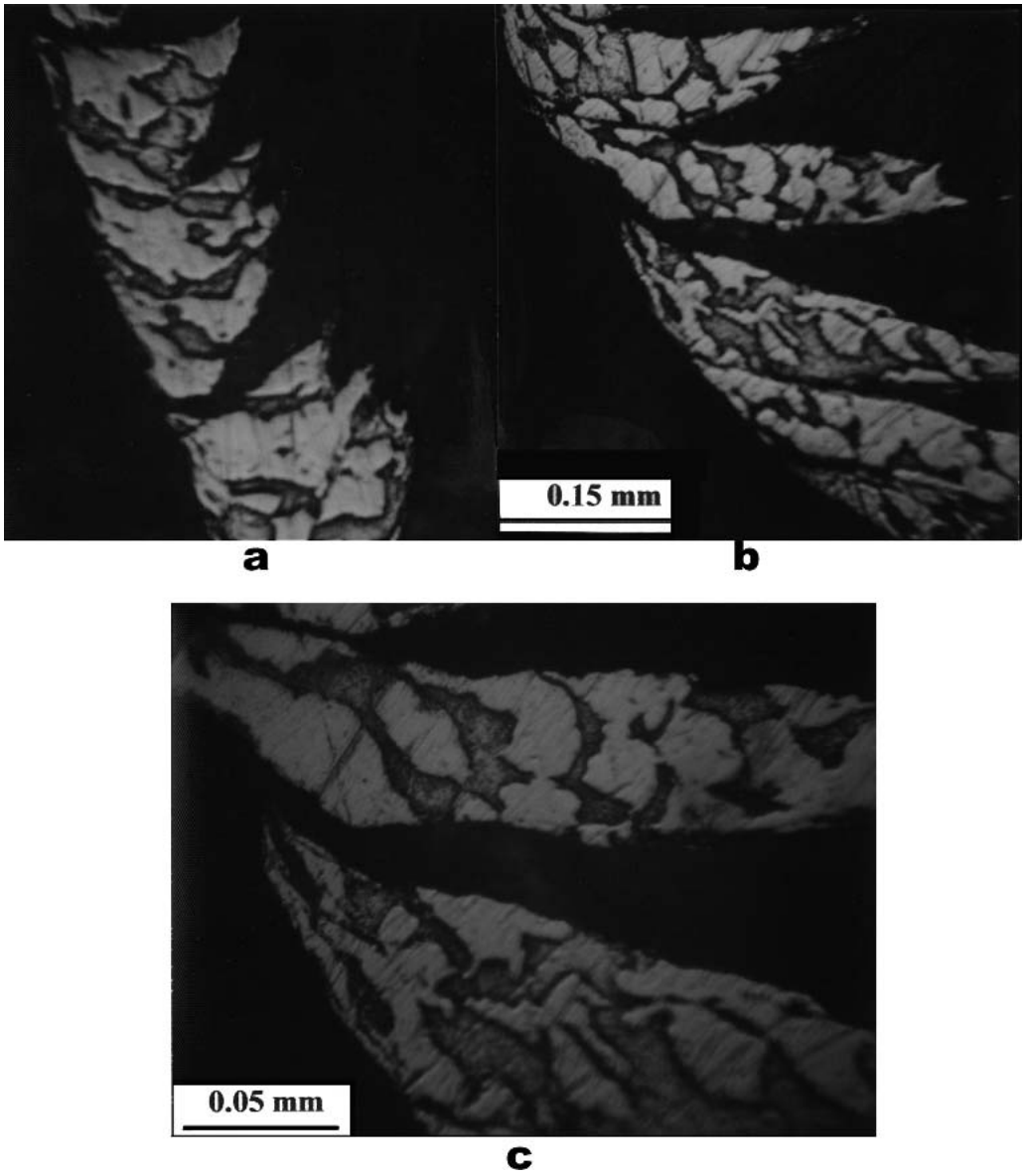

Fig. 6 **(a)** Segmented and **(b)** intensively fractured chip morphology without characteristic flow zone; **(c)** detail of Fig. 6(b) in the vicinity of the shear zone (depth of cut: 3.0 mm, feed rate: 0.25 mm/rev, cutting speed: 0.165 m/s)

References

1. *2000 Annual Book of ASTM Standards,* Copper and Copper Alloys, ASTM, West Conshohocken, PA, *2.01,* p. 601.
2. A. Gulyaev: *Physical Metallurgy,* Mir Publishers, Moscow, U.S.S.R., 1980, Vol. II (in English).
3. G. Pantazopoulos: *Copper Alloy Specifications, Colloquium of Greek Brass Manufacturers,* Athens, Greece, May 23, 2001 (in Greek).
4. K. Laue and H. Stenger: *Extrusion-Processes-Machinery-Tooling,* ASM International, Materials Park, OH, 1981.
5. R. Higgins: *Engineering Metallurgy-Applied Physical Metallurgy,* 6th ed., Arnold, London, United Kingdom, 1998.
6. L. Guillet: *Les Alliages de Cuivre,* Paris, France, 1925 (in French).
7. L. Guillet: *Revue de Metallurgie,* 1924, *21*, p. 293 (in French).
8. E.M. Trent: *Metal Cutting,* 3rd ed., Butterworth-Heinemann, Oxford, UK, 1996.
9. S. Kuyucaka and M. Sahoox, "A Review of the Machinability of Copper-Base Alloys," *Can. Metall. Q.,* 1996, *35*(1), p. 1.
10. V.P. Astakhov, "A Treatise on Material Characterization in the Metal-Cutting Process, Part 2: Cutting as the Fracture of Workpiece Material," *J. Mater. Process. Technology,* 1999, *96*(1-3), p. 34.